

## **Sr-Nd isotope composition of the Bay of Bengal Sediments: Impact of Climate on Erosion in the Himalaya**

Gyana Ranjan Tripathy<sup>1\*</sup>, Sunil Kumar Singh<sup>1</sup>, Ravi Bhushan<sup>1</sup> and V. Ramaswamy<sup>2</sup>

<sup>1</sup>Geosciences Division, Physical Research Laboratory, Ahmedabad 380009, India

<sup>2</sup>National Institute of Oceanography, Dona Paula, Goa 403004, India

\* Corresponding Author (gyana@prl.res.in)

### **ABSTRACT**

A temporal high-resolution analysis of the Sr-Nd isotopic composition, the Fe, Al and V composition and the magnetic susceptibility (MS) has been carried out in a sediment core from the western Bay of Bengal to trace sedimentary sources. Significant variations of the Sr and Nd isotopic composition and corresponding MS and elemental Fe/Al and V/Al ratios are observed in the sediment core with depth (time) indicating variable contributions from sources. The observed changes in the sediment provenance correlate well with the climatic record of the region, highlighting the important influence of climate over erosion. Relatively lower  $^{87}\text{Sr}/^{86}\text{Sr}$  and higher  $\epsilon_{\text{Nd}}$  corresponding to the Last Glacial Maximum (LGM) suggests proportionally reduced sediment contribution from the Himalaya. Erosion rate over the Himalaya decreased during LGM due to combined influence of reduced intensity of the southwestern monsoon and larger extent of glaciations over the Higher Himalaya, the main source of sediments to the Bay of Bengal.

Key Words: Himalaya; Bay of Bengal; Erosion; Climate; Sr-Nd isotopes.

## 1. INTRODUCTION

The Bay of Bengal (BoB) receives sediments from various sources including the Himalaya, Trans-Himalayan plutonic belt (TPB; Mishmi Hills), Indo-Burman Ranges and the Peninsular India through the major rivers, the Ganga, Brahmaputra, Irrawaddy, Salween, Godavari, Mahanadi and the Krishna. In these river basins, erosion is regulated by both the southwest (summer) and the northeast (winter) monsoons. There are evidences to show that the intensity of these monsoons varied over millennial timescale (Duplessy, 1982; Prell and Kutzbach, 1987; Sarkar *et al.*, 1990; Tiwari *et al.*, 2005; Herzsich, 2006). These variations in turn have the potential to influence the erosion pattern over the source regions and the sediment delivery to the BoB. Therefore, the variations in the sources of sediments deposited in the BoB hold clues to changes in the monsoon intensity.

In earlier studies, temporal variations in the provenance of sediments of the BoB have been tracked using Sr-Nd isotopes (France-Lanord *et al.*, 1993; Colin *et al.*, 1999; Pierson-Wickmann *et al.*, 2001; Ahmad *et al.*, 2005; Kessarkar *et al.*, 2005; Galy *et al.*, 2008). Over Ma time scale, the sources of sediments to the BoB have remained roughly the same since the Miocene (Bouquillon *et al.*, 1990; France-Lanord *et al.*, 1993). The sources are dominated by contributions from the Higher Himalaya (HH) with subordinate supply from the Lesser Himalaya (LH). However, on millennial timescale, there are evidences of variations in the provenance of sediments in the BoB related to climatic changes (Colin *et al.*, 1999; Goodbred, 2003; Ahmad *et al.*, 2005; Bookhagen *et al.*, 2005, 2006; Kessarkar *et al.*, 2005; Clift *et al.*, 2008; Rahaman *et al.*, 2009). This is consistent with the important role that climate has on the present-day erosion over the Himalaya, with most of sediments delivered to the BoB by rivers during the southwest monsoon (Islam *et al.*, 1999; Goodbred, 2003). In contrast, some of the studies carried out in the Nepal Himalaya (Burbank *et al.*, 2003), have decoupled climate and erosion and have highlighted the important control of tectonics on erosion. Compared to the Himalaya, there has been paucity of information on the paleo-erosion pattern of the Peninsular India river basins and their controlling factors. Based on clay mineralogy and Sr-Nd isotopes of marine sediments from the south-west margin of India, Kessarkar *et al.* (2003) concluded that these sediments are mainly from the Peninsular India and the Himalaya (Indus basin) and that their provenances and transport pathways remained the same during the late Pleistocene and Holocene.

These limited information on the monsoon-erosion relation in the Himalaya and the Peninsular India regions, warrant a detailed study. The western Bengal fan receives sediments predominantly from the Himalaya and the Peninsular India and hence it can be used to investigate the past erosion pattern of

these source regions. In the present study, efforts are made to track the provenances of the sediments from western BoB and their variations before, during and after the Last Glacial Maximum (LGM hereafter) and to identify the processes controlling the variations, based on sediment magnetic susceptibility (MS), chemical (Fe/Al and V/Al ratios) and Sr and Nd isotope compositions.

## 2. MATERIALS AND METHODS

The samples for this study are from a 12.8 m long piston core (SK187/PC33) collected from the western BoB (16° 16' N, 84° 30' E; Fig. 1;) during the 187<sup>th</sup> expedition of the ORV *Sagar Kanya*. The core was raised from an abyssal plain at a water depth of 3003 m (Fig. 1). Immediately after recovery the core was subjected to non-invasive measurements using a Geotek® Multi-Sensor Core Logger. Continuous down-core measurements were made of P-Wave velocity, whole core bulk density using gamma-ray attenuation, magnetic susceptibility and non-contact electrical resistivity. The core logs showed the core to be turbidite free. The lithology is mainly silty-clay and it does not show any significant changes with depth. The core location presently receives sediments mainly from the Himalaya and the Peninsular India. The Sr and Nd isotopic compositions of these two source regimes are distinctly different (Fig. 1; Table 1) and hence, temporal changes in the provenance of sediments and/or in their relative contributions should be reflected in their Sr and Nd isotope composition.

The depth-age relation for the core SK187/PC33 has been constrained using <sup>14</sup>C ages of bulk inorganic carbonates. The low abundance of carbonates in the sediment samples required processing of ~100 grams of bulk sediment samples for <sup>14</sup>C analysis (Bhushan *et al.*, 1994). Briefly, the dried sediments were treated with H<sub>3</sub>PO<sub>4</sub> in vacuum to convert the carbonate to CO<sub>2</sub>. From the CO<sub>2</sub>, benzene was synthesized for <sup>14</sup>C measurements and the <sup>14</sup>C activities were assayed using a low background liquid scintillation counter (Bhushan *et al.*, 1994). The calculated <sup>14</sup>C ages (Table 2) were calibrated using Calib 5.2 (Stuiver and Reimer, 1993) with a reservoir age correction of  $\Delta R = -60 \pm 50$  (Dutta *et al.*, 2001).

The magnetic susceptibility of the sediments was measured at ~10 cm depth interval using a MS2 Bartington magnetic susceptibility meter calibrated at 0.47 kHz frequency (Kessakar *et al.*, 2005). Abundances of Al, Fe and V were measured using an ICP-AES (Jobin-Yvon, Ultima) after dissolving the water-washed sediments by repeated treatment with HF-HCl-HNO<sub>3</sub>. The Sr and Nd concentrations and their isotopic compositions were measured in the silicate fraction of the sediments (Singh *et al.*,

2008) at ~50 cm intervals. Sediment samples were decarbonated by treating them with 0.6 N HCl at ~70°C followed by washing with distilled water. Initially, there were concerns about the effectiveness of the procedure in completely decarbonating the sediments, particularly samples with high CaCO<sub>3</sub> (e.g. 221-223, 440-442, 899-901 cmbsf; Tripathy *et al.*, 2008). Therefore, the high carbonate samples were reanalyzed after treating them one more time with 0.6 N HCl. The decarbonated and washed samples were ashed at 600°C to combust the organic matter. The residue (silicate phase), spiked with <sup>84</sup>Sr and <sup>150</sup>Nd, was digested with HF, HCl and HNO<sub>3</sub>. The samples were brought to complete solution and pure fractions of Sr and Nd were separated from the solution using conventional column chromatography (Singh *et al.*, 2008). The Sr and Nd isotope measurements were carried out using an ISOPROBE-T TIMS in static multi-collection mode. Sr and Nd data were normalized using <sup>86</sup>Sr/<sup>88</sup>Sr (=0.1194) and <sup>146</sup>Nd/<sup>144</sup>Nd (=0.7219) respectively. The average <sup>87</sup>Sr/<sup>86</sup>Sr ratio of standard NBS 987 during the period of study was 0.710229±0.000014 (1σ, n=85) and <sup>143</sup>Nd/<sup>144</sup>Nd for JNdi-1 Nd standard was 0.512102±0.000008 (1σ, n=13), within the recommended values. The differences in Sr and Nd isotopic ratios measured in replicates are insignificant compared to the range of values measured in the sediment (Table 3A). The total procedural blank for Sr and Nd were orders of magnitude lower than total Sr and Nd processed.

### 3. RESULTS

The concentrations of Al, Fe and V in total sediments of the core SK187/PC33 are given in Table 3A. The concentrations of Al, Fe and V vary from 2.5 to 9.2 wt%, 1.8 to 6.5 wt% and 30 to 130 µg/g respectively and show significant depth (temporal) variations. The MS of the core SK187/PC33 (Table 3B) ranges from 14 to 68 10<sup>-8</sup> m<sup>3</sup>/kg (Table 3B), comparable to earlier reported values for western BoB sediments (Kessarkar *et al.*, 2005).

The Sr, Nd concentrations in the silicate fraction and their <sup>87</sup>Sr/<sup>86</sup>Sr and ε<sub>Nd</sub> values also show significant variations with depth (Fig. 2; Table 3A). The abundances of Sr and Nd vary from 43 to 172 µg/g and from 13 to 63 µg/g respectively whereas the <sup>87</sup>Sr/<sup>86</sup>Sr ratios vary from 0.72528 to 0.75732 and ε<sub>Nd</sub> from -21.1 to -13.7 (Table 3A). The Sr isotope composition of these sediments is very radiogenic with values generally exceeding 0.735 (Table 3A), with corresponding ε<sub>Nd</sub> values often less than (-15). These values are within the range of isotopic composition of various sources supplying sediments to the core site (Fig. 3), though a dominance of the Himalayan source, as supplied by the Lower Meghna,

exists (see Discussion). Among the 36 samples analysed for Sr and Nd isotopic composition, two samples at depths of 222, 440 cmbsf show a sharp decrease in the  $\epsilon_{Nd}$  (and increase in  $^{87}Sr/^{86}Sr$  ratios) compared to samples from adjacent depths (Table 3A). The cause for these  $\epsilon_{Nd}$  and  $^{87}Sr/^{86}Sr$  anomalies is unclear. It may be the result of a unique event, such as significant sediment delivery during flood events from a tributary flowing through lithology with low  $\epsilon_{Nd}$  and  $^{87}Sr/^{86}Sr$  such as the Mahanadi and Pennar rivers draining Archean crust. These two samples have not been considered in the analysis of the isotope data to determine their general trend with depth (Fig. 2).

## 4. DISCUSSION

### 4.1 $^{87}Sr/^{86}Sr$ and $\epsilon_{Nd}$ in contemporary sediment sources to the BoB

The different sediment sources to the BoB show characteristic Sr and Nd isotopic compositions (Fig. 1, Table 1). For example, Himalayan rivers (such as the Ganga) supply sediments with highly radiogenic Sr and less radiogenic Nd compared to that of the sediments from the TPB, the Indo-Burmese ranges, the Arakan mountains and the Deccan Plateau, which are less radiogenic in Sr and more radiogenic in Nd (Table 1, Fig. 1; France-Lanord *et al.*, 1993; Colin *et al.*, 1999, 2006; Galy and France-Lanord, 2001; Singh and France-Lanord, 2002; Singh *et al.*, 2008; Ahmad *et al.*, 2009). The Godavari and the Krishna rivers drain the basaltic terrain of the Deccan traps upstream and the Archean cratons downstream. Therefore, the Sr and Nd isotopic composition of these river sediments (0.720 to 0.730 and -12.0 to -18.2 respectively; Ahmad *et al.*, 2009) depend on the relative contribution from these two sources. The representative Sr, Nd isotope compositions for the Archean crust (Fig. 1) used in this study are 0.716 and -25 respectively, compiled from earlier studies (Kessarkar *et al.*, 2003, 2005).

### 4.2 Temporal variations in the erosion pattern of Himalaya and Peninsular river basins of India

#### 4.2.1 Depth-Age model

The availability of an age-depth model for the SK187/PC33 core is a prerequisite to infer the temporal variations of the sources supplying sediments to the core location. The depth-age model has been established based on  $^{14}C$  of total inorganic carbon. The age distribution with depth in the core suggests that the LGM (18-21 ka) occurs at the depth range of ~600-700 cmbsf. The sedimentation rate of the core varies with depth with the lowest value at around LGM (460-620 cmbsf; 0.2 mm/yr) and about an order of magnitude higher (2.7 mm/yr) following the LGM (320-460 cmbsf). Similar pattern in

sedimentation, with high rates following the LGM have also been reported by Kessarkar *et al.* (2005) and Galy *et al.* (2008).

Since the  $^{14}\text{C}$  analyses were made in bulk carbonates, there could be an overestimation of the ages due to potential contribution of dead carbon from detrital carbonates. Earlier studies on  $^{14}\text{C}$  measurements in coarse and fine fractions of bulk carbonates showed that the finer fractions (comprising primarily of carbonate powder and nanoplanktons) were generally older than the coarser fractions (mature forams) by  $\sim 3$  ka (Sarkar, 1989; Sarkar *et al.*, 1990). The older age in the finer fraction was attributed to incorporation of dead detrital carbonates. Subsequently, Tiwari *et al.* (2005) by comparing  $\delta^{18}\text{O}$  spike in two cores, one dated by AMS on forams and the other (near-by core) by  $^{14}\text{C}$  on total carbonates, suggested that the age differ by  $\sim 3$  ka, the AMS dates being younger. An independent estimation of age correction can be obtained from the inorganic carbon contents of sediment sources and that in the SK187/PC33 core. The average carbonate content (expressed as  $\text{CaCO}_3$ ) is 8.6% in the five sections of SK187/PC33 analysed for  $^{14}\text{C}$ , compared to  $\sim 3\%$  in the Lower Meghna sediments (Galy and France-Lanord, 2001). Dilution of SK187/PC33 carbonates with the dead riverine carbonate would overestimate the age by  $\sim 3.5$  ka. The comparison of the pattern of MS profiles of the core analyzed in this study with that in an AMS  $^{14}\text{C}$  dated core from the western BoB (Kessarkar *et al.*, 2005), provides another approach to constrain the age-depth model. This approach essentially uses MS as a stratigraphic marker (Ninkovich *et al.*, 1966; Bloemendal *et al.*, 2005). Matching the prominent changes in the MS profiles in the top layers of the two cores (assuming that they are synchronous) indicates that the bulk carbonate ages of SK187/PC33 are older by  $\sim 4$  ka. The AMS dated western BoB core (Kessarkar *et al.*, 2005) had an age reversal at  $\sim 100$  cm, therefore the MS pattern of the two cores below this depth are not compared. In this study, samples having comparable calcium carbonate content ( $\sim 8\%$ ) were analyzed for  $^{14}\text{C}$  chronology so that the level of correction due to presence of detrital carbonate could be similar. Thus, based on available evidences, the bulk radiocarbon ages measured in the study could be  $\sim 3$ - $4$  ka older than actual ages. This suggests that the depositional age of the sample at depth 621 cmbsf, for which the measured  $^{14}\text{C}$  calendar age is  $\sim 24$  ka (Table 2), could be about 20 ka representing the LGM. In addition to the five samples in Table 2 one sample from 222 cmbsf depth with high  $\text{CaCO}_3$  ( $\sim 50\%$ ) content was also analyzed for  $^{14}\text{C}$ . This sample yielded an age of  $22000 \pm 600$  yr (PRLCH-724) significantly different that expected based on the age-depth model of the sample in Table 2. It is worth mentioning here that this sample also has anomalous  $^{87}\text{Sr}/^{86}\text{Sr}$  and  $\epsilon_{\text{Nd}}$  values (Table 3; Fig. 3). As a result, this data is not included for the depth-age relation.

#### 4.2.2 Temporal variations in geochemical and Sr-Nd isotopic signatures in the BoB sediments

The depth profiles of Sr and Nd isotope compositions of the core show significant temporal variations (Fig. 2). The range in  $^{87}\text{Sr}/^{86}\text{Sr}$  (0.725-0.757) and  $\epsilon_{\text{Nd}}$  (-13.7 to -16.9) indicate the dominance of the Himalayan source with minor contributions from the Peninsular Indian regions (Fig. 3). The  $^{87}\text{Sr}/^{86}\text{Sr}$  and  $\epsilon_{\text{Nd}}$  of the SK187/PC33 sediments (Table 3A) are bracketed by sediments from the Ganga, Brahmaputra and rivers from the Peninsular India and overlap with a few available data of the Lower Meghna (combined flow of the Ganga and the Brahmaputra in Bangladesh) indicating these rivers to be the major sediment supplier to the core site (Fig. 3).

The Sr-Nd isotopes depth profiles (Fig. 2) show a striking change in isotopic compositions around 600 cmbsf. Considering the age model of the sediment core, this major change in  $^{87}\text{Sr}/^{86}\text{Sr}$  and  $\epsilon_{\text{Nd}}$  coincide with the LGM. The  $^{87}\text{Sr}/^{86}\text{Sr}$  of the samples during LGM is  $\sim 0.725$  compared to their interglacial values of  $\sim 0.745$  (Fig. 2). The less radiogenic  $^{87}\text{Sr}/^{86}\text{Sr}$  of the sediments during LGM indicate a relatively reduced supply of sediments from the Himalayan rivers, particularly that of the Ganga (which is characterized by a highly radiogenic Sr signature; Table 1) compared to that during pre- and post-LGM relative to the Peninsular Indian rivers. This inference based on the  $^{87}\text{Sr}/^{86}\text{Sr}$  data is also supported from the trend of  $\epsilon_{\text{Nd}}$  values which shows a broad hump ( $\sim -14$ ) during the LGM compared to pre- and post-LGM values ( $-16$ ; Fig. 2). The concomitant changes in both  $^{87}\text{Sr}/^{86}\text{Sr}$  and  $\epsilon_{\text{Nd}}$  argue in favor of provenance changes and not due to particle sorting/weathering processes (*c.f.* Walter *et al.*, 2000; Tutken *et al.*, 2002; Colin *et al.*, 2006).

Similar to Sr-Nd isotopic signatures, the Fe/Al and V/Al ratios and MS (Fig. 4) of the sediment core also show significant variations with depth (time) indicating changes in relative proportion of sediments supplied from various sources. The Sr, Nd isotopes-based inference that the sediment contribution to the core site from the Himalayan source is relatively diminished during LGM is also confirmed by the V/Al and Fe/Al ratios. Distinctly higher V/Al and Fe/Al ( $(60-70) \times 10^{-4}$  and  $1.01 \pm 0.21$ ; Pattan *et al.*, 2008) characterize the rivers flowing through the Peninsular India compared to that of the G-B sediments (V/Al =  $(20-25) \times 10^{-4}$  and Fe/Al =  $0.44 \pm 0.10$ ; Pattan *et al.*, 2008). The humps in V/Al and Fe/Al profiles observed during LGM in SK187/PC33 (Fig. 4) attest to the relatively enhanced sediment supply from the Peninsular Indian rivers. This is also supported by the variation in the MS values. The magnetic susceptibility of sediments depends mainly on the abundance of detrital magnetic minerals present in them. The low carbonate content of the sediments from SK187/PC33 ensures that the magnetic susceptibility is a good tool to infer sediment provenance changes in the past (Bloemendal *et*

*al.*, 1993). Temporal variations of MS of the sediments show an increasing trend at around LGM (Fig. 4), suggesting higher abundances of ferromagnetic minerals (such as magnetite) and Fe-bearing silicates in the sediments. A very likely source for the high MS values during LGM is the relatively enhanced contribution of sediments from the Peninsular Indian region. This inference draws support from the significantly higher MS values for the fluvial sediments from Peninsular Indian regions compared to that from the sediments from the river basins of the Himalaya (Sangode *et al.*, 2007). The high MS value for the sediments from the Peninsular India particularly that for weathered products of the Deccan basalts, is due to the abundance of titanomagnetite with minor hematite (Courtillot *et al.*, 1986; Sager and Hall, 1990). A similar high MS value during LGM in the western Bengal fan was also reported by Sangode *et al.* (2001) and this change was attributed to weakening of sediment contribution from the Himalaya.

The above discussion, based on the isotope and trace element composition of the core SK187/PC33 along with its magnetic susceptibility reveal significant variations in the relative supply of sediments from the Himalaya and the Peninsular India over glacial-interglacial timescale. However, this conclusion rests on the assumption that the isotopic and chemical characteristics of these sources did not change since the LGM. This assumption seem to be valid for the G-B rivers as the Sr-Nd isotope ratios of the BoB sediments near the mouth of this river system has remained roughly the same since the LGM (Galy *et al.*, 2008). Rahaman *et al.* (2009), however, observed significant excursion in  $^{87}\text{Sr}/^{86}\text{Sr}$  (and  $\epsilon_{\text{Nd}}$ ) in sediments of the Ganga upstream, during the LGM. If this finding is typical of the entire G-B basin, then it would require that the relative proportion of G-B sediments in the SK187/PC33 core during LGM would have to be lower than that estimated based on their present-day  $^{87}\text{Sr}/^{86}\text{Sr}$  ratios.

The rivers draining the Peninsular India flow through multiple lithologies (Archean crust and Deccan traps) with their own distinct Sr-Nd isotope composition. Therefore, any change in the relative proportion of sediments from these two lithologies can alter the Sr-Nd isotopic signature of the peninsular sediments being delivered to the BoB. However, there is no evidence at present to suggest that the provenance of sediments of the Peninsular Indian rivers has changed in the past (Kessakar *et al.*, 2003). Increase in NE monsoon during LGM could enhance supply from the peninsular river basins. But this could result in a decrease of  $\epsilon_{\text{Nd}}$  unlike what has been observed in this study. Fig. 5 shows the Sr-Nd isotopic composition of the SK187/PC33 sediments along with the isotopic compositions of their dominant sources (*viz.* Higher Himalayan Crystallines, Lesser Himalayan silicates, Deccan traps and Archean). The dispersion of sediment data in the plot shows that their supply to the present core site is mainly from the HH, LH and the Deccan traps throughout the core length. The mixing curve among the



major sources show that ~30% of the sediments are supplied from the Deccan and rest from the HH and the LH. However, the sediments deposited during LGM, with lower  $^{87}\text{Sr}/^{86}\text{Sr}$  and high  $\epsilon_{\text{Nd}}$  values, have relatively larger contribution of sediments from the Peninsular India (both Deccan traps and Archean crust) sources. The relative proportion of Peninsular India sediments to the core site during LGM (~50%; Fig. 5) is almost twice that during the interglacial periods (~30%). The LGM shift in the SK187/PC33 sediments lean towards the mixing curve of Deccan and LH (Fig. 5), indicating relatively enhanced contribution from LH than that of HH during LGM. This is consistent with the results of Rahaman *et al.* (2009).

### 4.3 Impact of climate on continental Erosion

The excursions in Sr and Nd isotope composition of the sediments during LGM is compatible with the Asian monsoon strength variability (Prell and Kutzbach, 1987; Herzschuh, 2006). Climatic records show that during the LGM the intensity of the SW monsoon decreased (Prell and Kutzbach, 1987; Herzschuh, 2006) and that of NE monsoon increased (Duplessy, 1982; Prell *et al.*, 1990; Sarkar *et al.*, 1990; Tiwari *et al.*, 2005). The decrease in intensity of SW monsoon during LGM would limit its penetration into the Higher Himalaya, which is the dominant source of sediments to the Ganga and the Brahmaputra at present (Singh *et al.*, 2008). In addition, during the LGM the extent of glacial cover over the Higher Himalaya was larger (Owen *et al.*, 2002), further limiting physical erosion in the region. In contrast, there are evidences that during the LGM the NE monsoon was more intense (Duplessy, 1982; Prell and Kutzbach, 1987; Sarkar *et al.*, 1990; Tiwari *et al.*, 2005). This situation enhanced the sediment delivery from the rivers draining the Peninsular India and part of the drainage basin of the Brahmaputra (TPB), all of which have lower  $^{87}\text{Sr}/^{86}\text{Sr}$  and higher  $\epsilon_{\text{Nd}}$  (Fig. 1). Thus, the combination of decrease in SW monsoon and increase in NE monsoon during LGM contributed to decrease the relative proportion of sediments from the Himalaya to the core site, resulting in the  $^{87}\text{Sr}/^{86}\text{Sr}$  dip and  $\epsilon_{\text{Nd}}$  hump (Fig. 2). The link between monsoon activity and sediment supply is consistent with the results of Bookhagen *et al.* (2006), who have shown that intensification of monsoon enhances sediment supply from the HH. Further, the recent study of Rahaman *et al.* (2009) on a sediment core from the Ganga plain showed a decrease in sediment contribution from the HH to the Ganga plain during the LGM, supporting the observation of the current study.

An alternative, but unlikely hypothesis to explain the observed variation in the relative proportion of sediment from the Himalaya and the Peninsular India is to invoke the role of hydrography

and sea level changes in the Bay of Bengal in the dispersion of sediments. It can be argued that sediments from the Himalaya were transported directly to the central BoB during LGM due to lower sea level resulting in lower sediment proportion from the Himalaya at the core site. This proposition can be ruled out in case of sediments from the western BoB and particularly from the core site of SK187/PC33, as this core is from a water depth of ~3000 m and during LGM the Eastern Indian Coastal Current (EICC) was southwestward (Sarkar *et al.*, 1990; Schott and McCreary, 2001; Tiwari *et al.*, 2005). The EICC was directed N-S during LGM and hence, is expected to have focused more sediments from the Himalayan rivers to the western BoB compared to present-day, where the EICC is directed S-N. If so, the western BoB would have received higher proportion of Himalayan sediments during the LGM, which is contrary to the observations of the present study.

The variations in the Sr and Nd isotope composition of core SK187/PC33 attest an existing relation between past climatic changes and continental erosion. This hypothesis is also supported by earlier results on the variation of the Nd isotope composition of seawater and bulk sediments in the Bay of Bengal and in the Indian Ocean during the LGM and the Holocene (Burton and Vance, 2000; Stoll *et al.*, 2007; Gourelan *et al.*, 2010). Burton and Vance (2000) and Stoll *et al.* (2007) attributed changes in the Nd isotopic composition of seawater and bulk sediments during LGM to reduced erosional fluxes from the Himalaya caused by decrease in rainfall. This is consistent with the observation of this study.

Clift *et al.* (2008) investigated  $\epsilon_{Nd}$  of sediments from the Indus delta. Their results show variability consistent to those observed in this study i.e. decrease in  $\epsilon_{Nd}$  following LGM. This decrease can be attributed to relatively higher contribution of sediments from the Himalaya due to increase in monsoon intensity and decrease in snow cover. This interpretation is also supported by earlier observations of two-fold increase in the sediment supply from the Himalaya to the Bengal basin during these periods (Goodbred and Kuehl, 2000). In contrast to this, the results of Galy *et al.* (2008), based on Sr and Nd isotopic signatures of sediments from the channel-levee system in Bengal Fan, reported constancy in their sources since LGM. The reason behind this difference is unclear. One possible cause could be that the sampling site of Galy *et al.* (2008) is a channel-levee system, where sediments can undergo recycling. Further, the core site of Galy *et al.* (2008) receives sediments predominantly from G-B river, whereas the core SK187/PC33 receives sediments from the G-B rivers along with Peninsular Indian rivers and hence is able to better trace the signals of source variability.

The physical (MS), chemical and isotopic signature of SK187/PC33 showed a reduced Himalayan contribution to the BoB during LGM. It is interesting to note here that this observation

demonstrate the high efficiency of the Himalayan rivers in transferring the signal from their source (Himalaya) to the sink (BoB) and also indicates an insignificant time-lag between production of sediment in the Himalaya and their deposition in BoB. This observation hints that the residence time of the sediment of the Himalayan rivers in the plain seem to be very low, far less compared to that (~100 ka) proposed by Granet *et al.* (2007) based on the U-Th data of the sediments of the Gandak river.

## 5. CONCLUSIONS

The sediments from a core in the western Bay of Bengal are characterized by highly radiogenic Sr and low  $\epsilon_{Nd}$  values. This suggests relatively higher contribution of Himalayan-derived sediments to the core site than those from Peninsular India. The Sr and Nd isotope compositions show significant temporal variations suggesting considerable changes in the relative contributions from the Himalaya and the Peninsular India sources in the past. These variations in  $^{87}Sr/^{86}Sr$  and  $\epsilon_{Nd}$  support the hypothesis that during LGM, sediment contribution from the Himalaya was reduced due to decreased intensity of SW monsoon and increased extent of glacial cover over the High Himalaya.

## ACKNOWLEDGEMENTS

Discussions with S. Krishnaswami helped improving the manuscript significantly. Thanks to M. M. Sarin for logistic support. M. G. Yadav and J. P. Bhavsar helped during  $^{14}C$  measurements. Help of B. Srinivas and P. Kessarkar during geochemical and MS analyses is acknowledged. We thank Daniele Pinti, the associate (and vice) editor and two anonymous reviewers for their constructive comments and suggestions. Financial assistance was provided by the Ministry of Earth Sciences for collection of piston cores under the BENFAN project. This is NIO contribution No. xxxx.

## Reference:

Ahmad, S. M., Anil Babu, G., Padmakumari, V. M., Dayal, A. M., Sukhija and B. S., Nagabhushanam, P. (2005) Sr, Nd isotopic evidence of terrigenous flux variations in the Bay of Bengal: Implications of monsoons during the last ~34,000 years. *Geophys. Res. Lett.*, **32**, 1-4.

Ahmad, S. M., Padmakumari and Anil Babu, G. (2009) Strontium and neodymium isotopic compositions in sediments from Godavari, Krishna and Pennar rivers. *Curr. Sci.*, **97**, 1766-1769.

Bhushan R., Chakraborty, S. and Krishnaswami, S. (1994) Physical Research Laboratory (Chemistry) Radiocarbon Date list I. *Radiocarbon*, **36**, 251-256.

Bloemendal, J., King, J., Hunt, A., Demenocal, P. and Hayashida, A. (1993) Origin of the sedimentary magnetic record at Ocean drilling program sites on the Owen ridge, western Arabian sea. *J. Geophys. Res.*, **98**, 4199-4219.

Bloemendal, J., Liu, X. And Rolph, T. (1995) Correlation of the magnetic susceptibility stratigraphy of Chinese loess and the marine oxygen isotope record: chronological and palaeoclimatic implications. *Earth Planet. Sci. Lett.*, **131**, 371-380.

Bookhagen, B., Fleitmann, D., Nishiizumi, K., Strecker, M. R. and Thiede, R. C. (2006) Holocene monsoonal dynamics and fluvial terrace formation in the northwest Himalaya, India, *Geology*, **34**, 601-604.

Bookhagen, B., Thiede, R. C. and Strecker, M. R. (2005) Late Quaternary intensified monsoon phases control landscape evolution in the northwest Himalaya, *Geology*, **33**, 149-152.

Bouquillon, A., France-Lanord, C., Michard, A. and Tiercelin, J. J. (1990) Sedimentology and isotopic chemistry of the Bengal Fan sediments: the denudation of the Himalaya, *Proc., scientific results*, ODP, Leg 116, distal Bengal Fan, 43-58.

Burbank, D. W., Blythe, A. E., Putkonen, J., Pratt-Sitaula, B., Gabet, E., Oskin, M., Barros, A. and Ojha, T. P. (2003) Decoupling of erosion and precipitation in the Himalayas, *Nature*, **426**, 652-655.

Burton, K. W. and Vance, D. (2000) Glacial-interglacial variations in the neodymium isotope composition of seawater in the Bay of Bengal recorded by planktonic foraminifera, *Earth Planet. Sci. Lett.*, **176**, 425-441.

Clift, P. D., Giosan, L., Blusztajn, J., Campbell, I. H., Allen, C., Pringle, M., Tabrez, A. R., Danish, M., Rabbani, M. M., Alizai, C. A., Lückge A. (2008) Holocene erosion of the Lesser Himalaya triggered by intensified summer monsoon, *Geology*, **36**, 79-82.

Colin, C., Turpin, L., Bertaux, J., Desprairies, A. and Kissel, C. (1999) Erosional history of the Himalayan and Burman ranges during the last two glacial-interglacial cycles, *Earth Planet. Sci. Lett.*, **171**, 647-660.

Colin, C., Turpin, L., Blamart, D., Frank, N., Kissel, C. and Duchamp, S. (2006) Evolution of weathering patterns in the Indo-Burman Ranges over 280 kyr: Effects of sediment provenance on  $^{87}\text{Sr}/^{86}\text{Sr}$  ratios tracer, *Geochem. Geophys. Geosyst.*, **7**, doi:10.1029/2005GC000962.

Courtillot, V., Besse, J., Vandamme, D., Montigny, R., Jaeger, J. and Cappetta, H. (1986) Deccan flood basalts at Cretaceous/Tertiary boundary? *Earth Planet. Sci. Lett.*, **80**, 361-374.

Duplessy, J. C. (1982) Glacial to interglacial contrasts in the northern Indian Ocean, *Nature*, **295**, 494-498.

Dutta, K., Bhushan, R. and Somayajulu, B. L. K. (2001)  $\Delta R$  correction values for the northern Indian Ocean, *Radiocarbon*, **43**, 483-488.

France-Lanord, C., Derry, L. and Michard, A. (1993) Evolution of the Himalaya since Miocene time: Isotopic and sedimentologic evidence from the Bengal Fan, in *Himalayan Tectonics*, edited by P. J. Treloar and M. Searle, *Geol. Soc. Spec. Publ.*, **74**, 603–621.

Galy, A. and France-Lanord, C. (2001) Higher erosion rates in the Himalaya: Geochemical constraints on riverine fluxes, *Geology*, **29**, 23-26.

Galy, V., Francois, L., France-Lanord, C., Faure, P., Kudrass, H., Pailhol, F. and Singh, S. K. (2008) C4 plants decline in the Himalayan basin since the Last Glacial Maximum, *Quat. Sci. Rev.*, **27**, 1396-1409.

Goodbred, S. L., Jr. (2003) Response of the Ganges dispersal system to climate change: a source-to-sink view since the last interstade, *Sediment. Geol.*, **162**, 83-104.

Goodbred, S.L., Jr. and Kuehl, S.A. (2000) The significance of large sediment supply, active tectonism, and eustasy on margin sequence development: Late Quaternary stratigraphy and evolution of the Ganges-Brahmaputra delta. *Sediment. Geol.*, **133**, 227–248.

Gourlan, A., Meynadier, L., Allegre, C., Tapponnier, P., Birck, J. and Joron, J. (2010) Northern Hemisphere climate control of the Bengali rivers discharge during the past 4 Ma. *Quaternary Science Reviews* **29**, 2484-2498.

Granet, M., F., Chabaux, P., Stille, C., France-Lanord and Pelt, E. (2007) Time-series of sedimentary transfer and weathering processes from U-series nuclides : Clues from the Himalayan rivers. *Earth Planet. Sci. Lett.*, **261**, 389-406.

Herzschuh, U. (2006) Palaeo-moisture evolution in monsoonal Central Asia during the last 50,000 years, *Quat. Sci. Rev.*, **25**, 163-178.

<http://www.gemswater.org/atlas-gwq/table3-e.html>

Islam, M. R., Begum, S. F., Yamaguchi, Y. and Ogawa, K. (1999) The Ganges and Brahmaputra rivers in Bangladesh: Basin denudation and sedimentation, *Hydrol. Proc.*, **13**, 2907-2923.

Kessarkar, P. M., Rao, V. P., Ahmad, S. M., Patil, S. K., Anil Kumar, A., Anil Babu, G., Chakraborty, S. and Soundar Rajan, R. (2005) Changing sedimentary environment during the Late Quaternary: Sedimentological and isotopic evidence from the distal Bengal Fan, *Deep Sea Res.*, **52**, 1591-1615.

Kessarkar, P. M., Rao, V. P., Ahmad, S. M. and Anil Babu G. (2003) Clay minerals and Sr-Nd isotopes of the sediments along the western margin of India and their Implication for sediment provenance, *Mar. Geol.*, **202**, 55-69.

- Ninkovich, D., Opdyke, N., Heezen, B. and Foster, J. (1966) Palaeomagnetic stratigraphy, rates of deposition and tephrochronology in North Pacific deep-sea sediments. *Earth Planet. Sci. Lett.*, **1**, 476-492.
- Owen, L. A., Finkel, R. C. and Caffee, M. W. (2002) A note on the extent of glaciation throughout the Himalaya during the global Last Glacial Maximum, *Quat. Sci. Rev.*, **21**, 147-157.
- Pattan, J.N., G., Parthiban, C., Prakash Babu and N.H., Khadge (2008) A note on geochemistry of surface sediments from Krishna-Godavari basin, East coast of India. *J. Geol. Soc. India*. **71**, 107-114.
- Pierson-Wickmann, A.-C., Reisberg, L., France-Lanord, C. and Kudrass H. R. (2001) Os-Sr-Nd results from sediments in the Bay of Bengal: Implications for sediment transport and the marine Os record, *Paleoceanography*, **16**, 435-444.
- Prell, W. L., Hutson, W., Williams, D. F., Be, A. W. H., Geitzenauer, K. and Molino B. (1980) Surface circulation of the Indian Ocean during the last Glacial Maximum approximately 18,000 yr B.P., *Quat. Res.* **14**, 309– 336.
- Prell, W. L. and Kutzbach, J. E. (1987) Monsoon variability over the past 150, 000 years, *J. Geophys. Res.*, **92**, 8411-8425.
- Rahaman, W., Singh, S. K., Sinha, R. and Tandon, S. K. (2009) Climate control on erosion distribution over the Himalaya during the past ~100 ka, *Geology*, **37**, 559-562.
- Robinson, R.A.J., Bird, M. I., Oo, N. W., Lu, X. X., Hoey, T. B., Swe, A. and Tun, T. (2006) Reanalysis of the 19<sup>th</sup> century hydrology and sediment load dataset for the Irrawaddy River, Myanmar, *Geophys. Res. Abstracts*, **8**, 10097.
- Sager, W. and Hall, S. (1990) Magnetic properties of black mud turbidites from ODP Leg 116, Distal Bengal Fan, Indian Ocean. In: Proceedings of the ocean Drilling Programme, Scientific results (eds Cochran, J. et al.), **116**, 317-336.
- Sarkar, A. (1989) Oxygen and Carbon isotopes in Indian Ocean sediments and their Palaeoclimatic implications, Ph D. Thesis, Gujarat University, 55-57.
- Sarkar, A., Ramesh, R., Bhattacharya, S. K. and Rajagopalan, G. (1990) Oxygen isotope evidence for a stronger winter monsoon current during the last glaciation, *Nature*, **343**, 549-551.
- Sangode, S., Suresh, N. and Bagati T. (2001) Godavari source in the Bengal fan sediments: Result from magnetic susceptibility dispersal pattern. *Curr. Sci.*, **80**, 660-664.
- Sangode, S., Sinha, R., Phartiyal, B., Chauhan, O., Mazari, R., Bagati, T., Suresh, N., Mishra, S., Kumar, R. and Bhattacharjee, P. (2007) Environmental magnetic studies on some quaternary sediments of varied depositional settings in the Indian sub-continent. *Quat. Int.*, **159**, 102-118.

Schott, F. A., and J. P. McCreary Jr. (2001) The monsoon circulation of the Indian Ocean, *Prog. Oceanogr.*, **51**, 1 – 123.

Singh, S. K. and France-Lanord, C. (2002) Tracing the distribution of erosion in the Brahmaputra watershed from isotopic compositions of stream sediments, *Earth Planet. Sci. Lett.*, **202**, 645-662.

Singh, S. K., Rai, S. K. and Krishnaswami, S. (2008) Sr and Nd isotopes in River sediments from the Ganga basin: Sediment provenance and spatial variability in physical erosion, *J. Geophys. Res.*, **113**, F03006, doi:10.1029/2007JF000909.

Stoll, H. M., Vence, D. and Arevalos, A. (2007) Records of the Nd isotope composition of seawater from the Bay of Bengal: Implications for the impact of Northern Hemisphere cooling on ITCZ movement, *Earth Planet. Sci. Lett.*, **255**, 213-228.

Stuiver, M. and Reimer, P. J. (1993) Extended  $^{14}\text{C}$  data base and revised CALIB 3.0  $^{14}\text{C}$  age calibration program, *Radiocarbon*, **35**, 215-230.

Tiwari, M., Ramesh, R., Somayajulu, B. L. K., Jull, A. J. T. and Burr, G. S. (2005) Early deglacial (~19-17 ka) strengthening of the northeast monsoon, *Geophys. Res. Lett.*, **32**, 1-4.

Tripathy, G., Singh, S. and Ramaswamy, V. (2008) Tracking the provenance of sediments of the Bay of Bengal through their Sr concentration and  $^{87}\text{Sr}/^{86}\text{Sr}$ , Conference on “Terrestrial planets: Evolution through time”, India.

Tutken, T., Eisenhauer, A., Wiegand, B. and Hansen, B. T. (2002) Glacial-interglacial cycles in Sr and Nd isotopic composition of Arctic marine sediments triggered by the Svalbard/Barents Sea ice sheet, *Mar. Geol.*, **182**, 351-372.

Walter, H. J., Hegner, E., Diekmann, B., Kuhn, G. and Rutgers van der loeff, M. M. (2000) Provenance and transport of terrigenous sediment in the south Atlantic Ocean and their relations to glacial and interglacial cycles: Nd and Sr isotopic evidence, *Geochim. Cosmochim. Acta*, **64**, 3813-3827.

## Figure captions

**Figure 1.** Location of the sediment core SK187/PC33 (white circle marked) in the Bay of Bengal. The various sources of sediments to the core site with their characteristic  $^{87}\text{Sr}/^{86}\text{Sr}$  and  $\epsilon_{\text{Nd}}$  are also shown (Data Source: Colin *et al.*, 1999, 2006; Ahmad *et al.*, 2009; Singh *et al.*, 2008). Bathymetry data are from [http://www.bodc.ac.uk/data/online\\_delivery/gebco/](http://www.bodc.ac.uk/data/online_delivery/gebco/).

**Figure 2.** Depth profile of Sr and Nd isotope composition of sediments from the core SK187/PC33 (dots). The solid line is the 3-point moving average of the data. Data show a dip in  $^{87}\text{Sr}/^{86}\text{Sr}$  and a hump in  $\epsilon_{\text{Nd}}$  excursions at ~600 cmbsf coinciding with the Last Glacial Maximum. Two anomalous samples at depth ~220 and 440 cmbsf are not included. The squares in the figure represent the average Sr-Nd isotopic values for the contemporary Peninsular Indian river sediments (PEN; Ahmad *et al.*, 2009) and the combined flow (Lower Meghna) of G-B river sediments (Triangle (GB); Galy and France-Lanord, 2001).

**Figure 3.**  $^{87}\text{Sr}/^{86}\text{Sr}$  vs.  $\epsilon_{\text{Nd}}$  of the sediments from core SK187/PC33. The isotope composition of various sources contributing to these sediments is also given. The Sr and Nd isotope composition of SK187/PC33 sediments falls within the isotopic values of riverine sediments from the Himalaya and the Peninsular India. The two samples (encircled) having low  $\epsilon_{\text{Nd}}$  seem to be anomalous and could be deposited by flood events in particular rivers such as the Mahanadi or the Pennar flowing through an Archean crust with radiogenic Sr and unradiogenic Nd.

**Figure 4.** Depth profiles of magnetic susceptibility (MS), Fe/Al and V/Al ratios for the SK187/PC33 sediments. The higher values of MS, V/Al and Fe/Al during the LGM indicate a relatively lower contribution from the Himalaya. The solid line is the 3-point moving average of the data.

**Figure 5.** Sr and Nd isotopic mixing plot for the SK187/PC33 sediments along with isotopic values of their dominant sedimentary sources. The dominance of the Himalayan sources, particularly HH, is observed for most of the sediments from the SK187/PC33 core, whereas an enhanced contribution from the Deccan traps is mainly observed during the LGM. The hyperbolic curve shown is the mixing trend among the sources. The curvature of the curve plotted based on the average  $^{87}\text{Sr}/^{86}\text{Sr}$  and  $\epsilon_{\text{Nd}}$  ratios of the sources. The representative isotopic values for the sedimentary sources are from Singh *et al.* (2008), except for the TPB (Average of predominantly TPB flowing (Lohit and Dibang) river sediments; Singh and France-Lanord, 2002) and Archean terrains (Compiled from Kessarkar *et al.*, 2003, 2005).



Table 1: Basin characteristics and Sr, Nd isotopic composition of sediments at the outflow of major rivers contributing sediments to the BoB.

Basin	River	Major Litho-units	Area 10 <sup>6</sup> km <sup>2</sup>	Runoff mm/yr	Water discharge km <sup>3</sup> /yr	Sediment flux 10 <sup>6</sup> tons/yr	Sediments	
							<sup>87</sup> Sr/ <sup>86</sup> Sr	εNd
Himalaya	Ganga <sup>1,2</sup>	HH, LH	0.95	619	460	520	0.762 to 0.782	-16.1 to -18.1
	Brahmaputra <sup>1,3</sup>	HH, LH, TPB, Indo-Burmese Ranges	0.58	1087	630	540	0.721 to 0.749	-13.6 to -16.9
	Lower Meghna <sup>1</sup>		-	-	-	-	0.738 to 0.753	-14.8 to -17.4
Peninsular India	Mahanadi	Archean Crust	0.132	500	66	60	-	-
	Godavari <sup>4</sup> Krishna <sup>4</sup>	Deccan Trap, Archean Crust	0.31 0.252	350 266	92 67	170 16	0.720 to 0.730	-12.0 to -18.2
Indo-Burman Ranges	Irrawaddy <sup>5</sup>	Indo-Burmese Ranges, Arakan Mountains	0.414	1034	428	355 <sup>§</sup>	0.713	-10.7
	Salween	TPB, Indo-Burmese Ranges	0.325	649	211	337 <sup>§</sup>	-	-

Hydrological parameters from <http://www.gemswater.org/atlas-gwq/table3-e.html>; <sup>§</sup>Robinson *et al.*, 2006.  
Sr and Nd isotopic data for the sediment of the rivers at their outflow are from <sup>1</sup>Galy and France-Lanord, 2001; <sup>2</sup>Singh *et al.*, 2008; <sup>3</sup>Singh and France-Lanord, 2002; <sup>4</sup>Ahmad *et al.*, 2009; <sup>5</sup>Colin *et al.*, 1999.

Table 2:  $^{14}\text{C}$  ages of inorganic carbon from the core SK187/PC33.

<b>Sample code</b>	<b>Depth (cmbsf)</b>	<b>Radiocarbon ages (yr BP)</b>	<b>Calibrated <math>^{14}\text{C}</math> age (yr BP)</b>
<b>PRLCH-725</b>	54±17	7788 ± 295	8361 ± 953
<b>PRLCH-766</b>	281±16	13573 ± 302	15727 ± 1277
<b>PRLCH-770</b>	316±8	13964 ± 325	16171 ± 1333
<b>PRLCH-776</b>	466±23	14286 ± 355	16728 ± 1572
<b>PRLCH-777</b>	621±30	21242 ± 610	24840 ± 1613

Table 3A: Elemental abundances<sup>§</sup>, Sr, Nd concentrations and their isotope composition<sup>@</sup> in the sediment core SK187/PC33.

Depth (cmbfsf)	Al (%wt)	Fe	V (µg/g)	Sr (µg/g)	<sup>87</sup> Sr/ <sup>86</sup> Sr	Nd (µg/g)	εNd
10-12	8.96	6.54	130	56	0.74041	17	-15.5
18-20	7.44	4.05	90	87	0.75051	22	-16.9
28-30	8.83	6.42	125	57	0.74089	18	-14.6
109-111	7.95	6.22	119	58	0.74212	19	-15.4
149-151	8.85	5.63	115	59	0.74457	18	-15.9
201-203	8.47	4.88	106	43	0.74522	19	-15.8
221-223	2.50	2.17	30	73	0.75732	63	-21.1
249-251	8.82	5.78	112	60	0.73759	13	-15.7
300-302	7.89	5.57	108	69	0.73528	13	-15.8
320-322	6.28	3.97	77	98	0.73483	19	-15.1
340-342	<i>n.a.</i>	<i>n.a.</i>	<i>n.a.</i>	49	0.74273	17	-15.8
350-352	8.63	4.69	78	82	0.75150	24	-15.8
360-362	<i>n.a.</i>	<i>n.a.</i>	<i>n.a.</i>	43	0.74621	14	-15.6
400-402	6.41	3.87	78	87	0.73768	19	-15.3
440-442	2.84	1.84	34	84	0.74422	24	-19.6
450-452	8.27	4.97	105	82	0.73475	19	-14.9
490-492	<i>n.a.</i>	<i>n.a.</i>	<i>n.a.</i>	58	0.74248	17	-16.5
500-502	8.22	4.47	99	71	0.75515	21	-16.5
510-512	<i>n.a.</i>	<i>n.a.</i>	<i>n.a.</i>	54	0.74009	17	-15.4
550-552	6.15	2.52	49	123	0.73594	18	-14.6
600-602	6.80	4.42	104	104	0.72861	37	-15.0
650-652	7.30	4.88	115	99	0.72528	19	-13.7
700-702	7.77	4.84	112	101	0.72750	19	-14.5
750-752	7.75	3.84	83	127	0.73573	20	-14.5
800-802	8.13	4.86	89	83	0.73284	20	-13.8
849-851	6.81	3.57	79	101	0.73638	24	-15.5
889-891	<i>n.a.</i>	<i>n.a.</i>	<i>n.a.</i>	54	0.73062	13	-14.9
899-901	5.57	3.69	56	68	0.74026	17	-17.1
909-911	<i>n.a.</i>	<i>n.a.</i>	<i>n.a.</i>	61	0.73310	16	-14.0
949-951	7.87	4.82	103	97	0.73679	<i>n.a.</i>	<i>n.a.</i>
999-1001	4.55	2.63	53	89	0.73851	21	-14.9
1049-1051	8.07	4.46	94	111	0.74016	21	-15.5
1099-1101	8.72	4.98	103	105	0.73865	18	-15.9
1149-1151	7.55	3.68	73	145	0.73334	27	-14.7
1199-1201	6.00	1.86	35	172	0.72903	13	-14.5
1219-1221	9.19	4.87	96	116	0.73669	23	-14.8

*n.a.*: Not Analyzed.

<sup>§</sup> The concentrations of Al, Fe and V are measured in bulk sediments.

<sup>@</sup> Sr, Nd and their isotopic compositions are measured in their silicate fractions. Errors on Sr and Nd isotopic compositions are better than 10 ppm.

Table 3B: Magnetic susceptibility (MS) of sediments from the core SK187/PC33\*.

Depth	MS $10^{-8} \text{ m}^3/\text{kg}$	Depth	MS $10^{-8} \text{ m}^3/\text{kg}$	Depth	MS $10^{-8} \text{ m}^3/\text{kg}$
6-8 cm	25.6	424-426 cm	22.1	833-835 cm	23.7
12-14 cm	29.7	452-454 cm	18.7	835-837 cm	24.6
22-24 cm	33.9	476-478 cm	29.9	837-839 cm	23.6
30-32 cm	33.7	510-512 cm	25.0	855-857 cm	26.5
38-40 cm	27.4	512-514 cm	24.6	857-859 cm	25.5
50-52 cm	24.2	556-558 cm	34.0	931-933 cm	19.2
56-58 cm	20.7	568-570 cm	33.0	933-935 cm	21.8
70-72 cm	23.5	578-580 cm	52.0	935-937 cm	22.3
82-83 cm	36.8	592-594 cm	35.1	937-939 cm	20.0
91-93 cm	34.5	612-614 cm	24.6	941-943 cm	20.4
97-99 cm	25.0	624-626 cm	34.7	943-945 cm	20.5
109-111 cm	33.3	632-634 cm	31.1	959-961 cm	19.8
121-123 cm	30.9	644-646 cm	37.5	961-963 cm	26.8
173-175 cm	18.4	648-650 cm	36.3	967-969 cm	27.0
183-185 cm	17.7	660-662 cm	21.7	969-971 cm	24.0
185-187 cm	17.9	670-672 cm	28.3	1001-1003 cm	33.0
211-213 cm	14.0	678-680 cm	23.1	1019-1021 cm	45.3
221-223 cm	15.3	690-692 cm	46.6	1029-1031 cm	24.0
262-264 cm	14.7	700-702 cm	43.3	1049-1051 cm	22.5
268-270 cm	20.1	710-712 cm	26.3	1077-1079 cm	18.3
274-276 cm	15.3	732-734 cm	23.4	1081-1083 cm	17.6
284-286 cm	17.1	760-762 cm	35.6	1099-1101 cm	18.0
300-302 cm	22.2	770-772 cm	30.4	1109-1111 cm	22.6
308-310 cm	19.8	790-792 cm	23.1	1127-1129 cm	28.4
316-318 cm	14.3	798-800 cm	24.3	1139-1141 cm	21.4
336-338 cm	14.2	810-812 cm	40.0	1151-1153 cm	68.0
346-348 cm	20.3	820-821 cm	34.0	1187-1189 cm	47.1
362-364 cm	16.9	821-823 cm	25.9	1201-1203 cm	46.8
372-374 cm	20.4	827-829 cm	20.6	1211-1213 cm	22.3
402-404 cm	23.3	831-833 cm	22.2	1217-1219 cm	30.4

\*measured at frequency 0.47 kHz

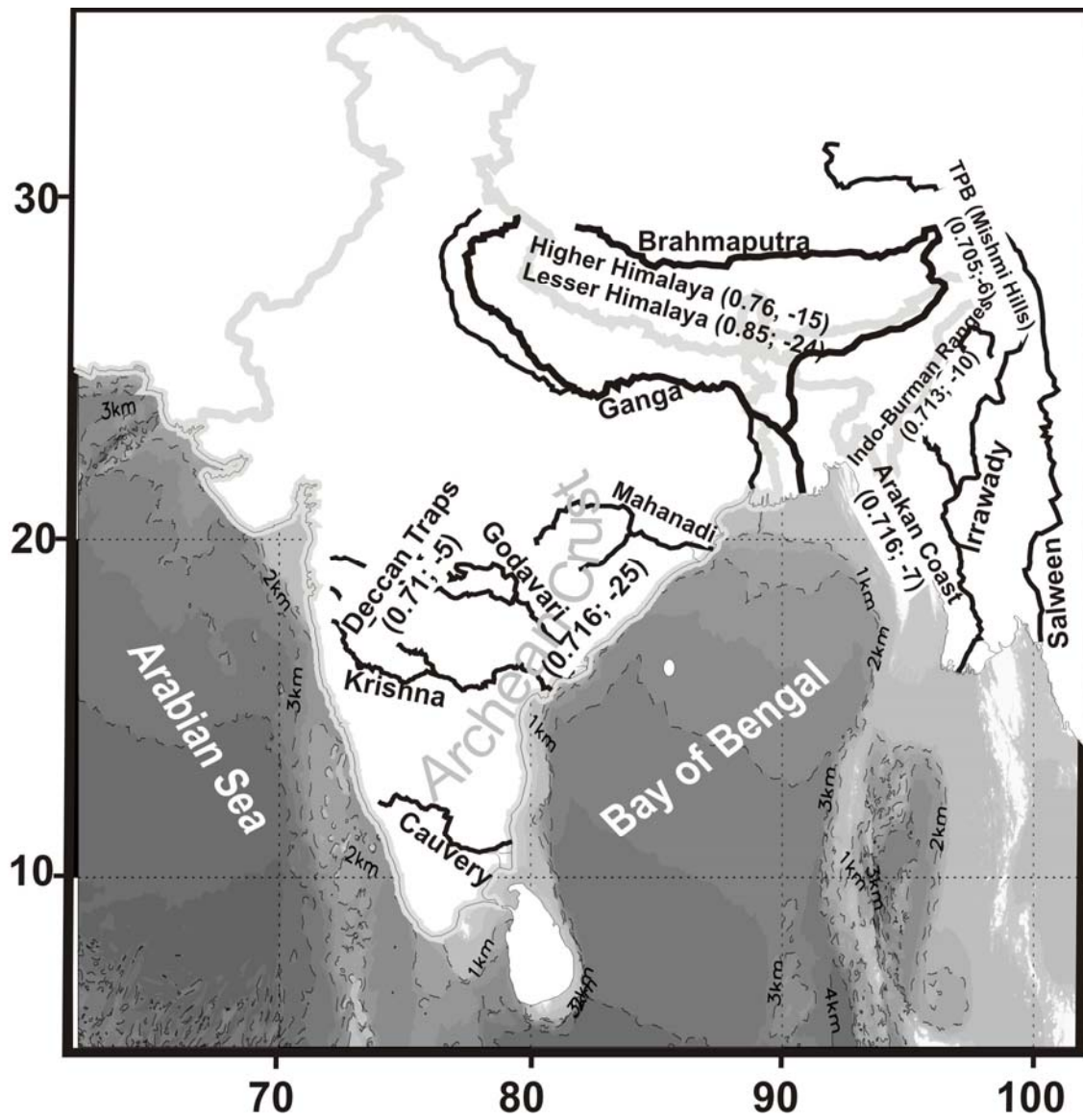


Fig. 1

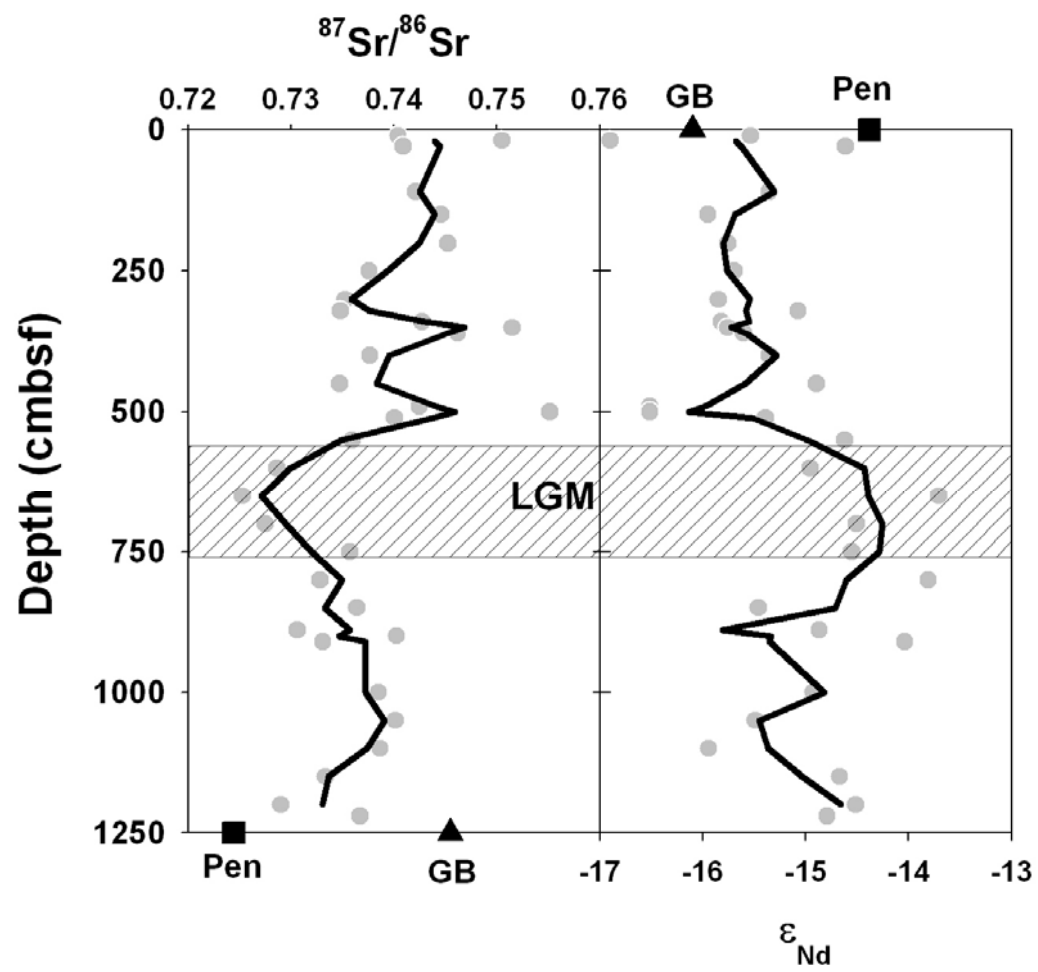


Fig. 2

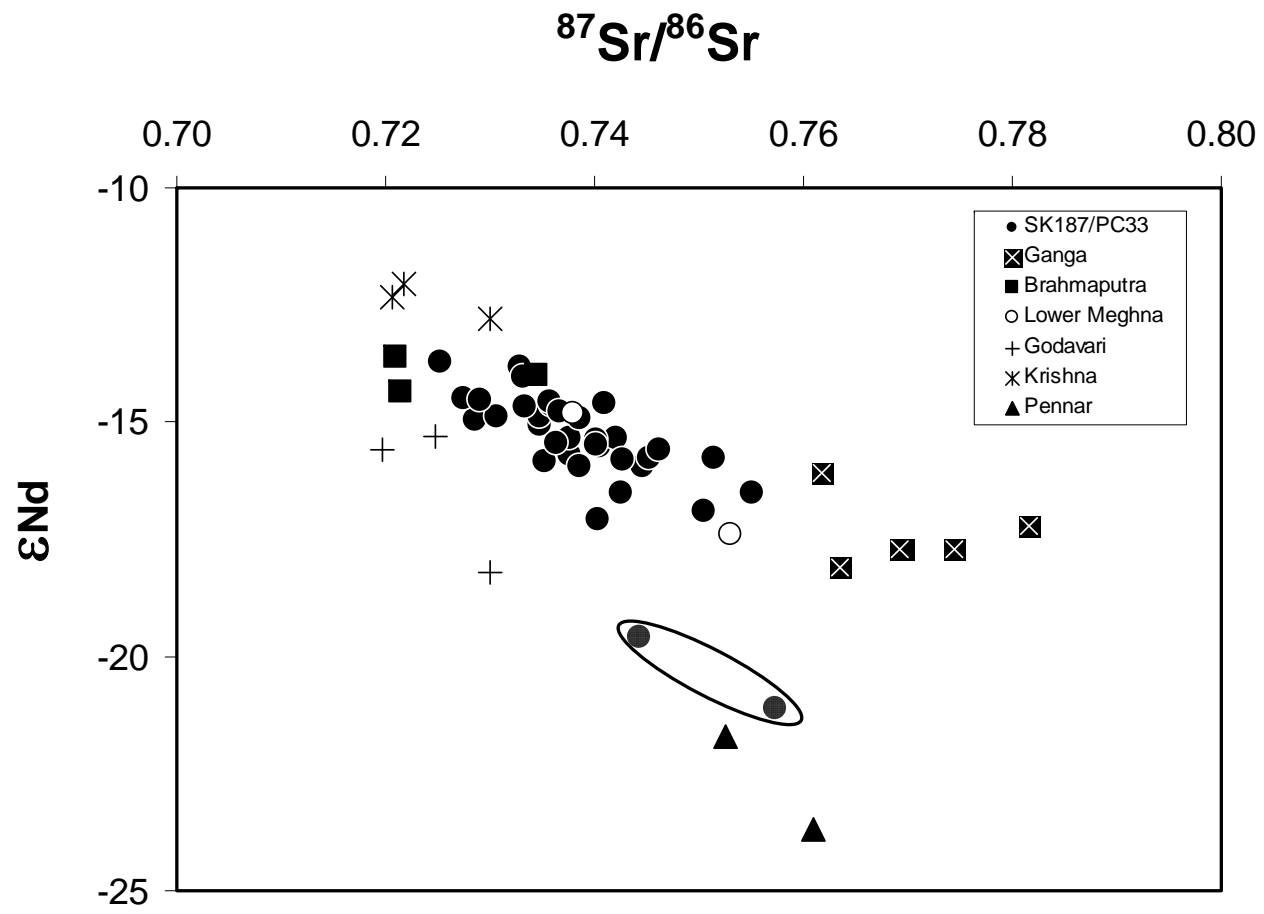


Fig. 3

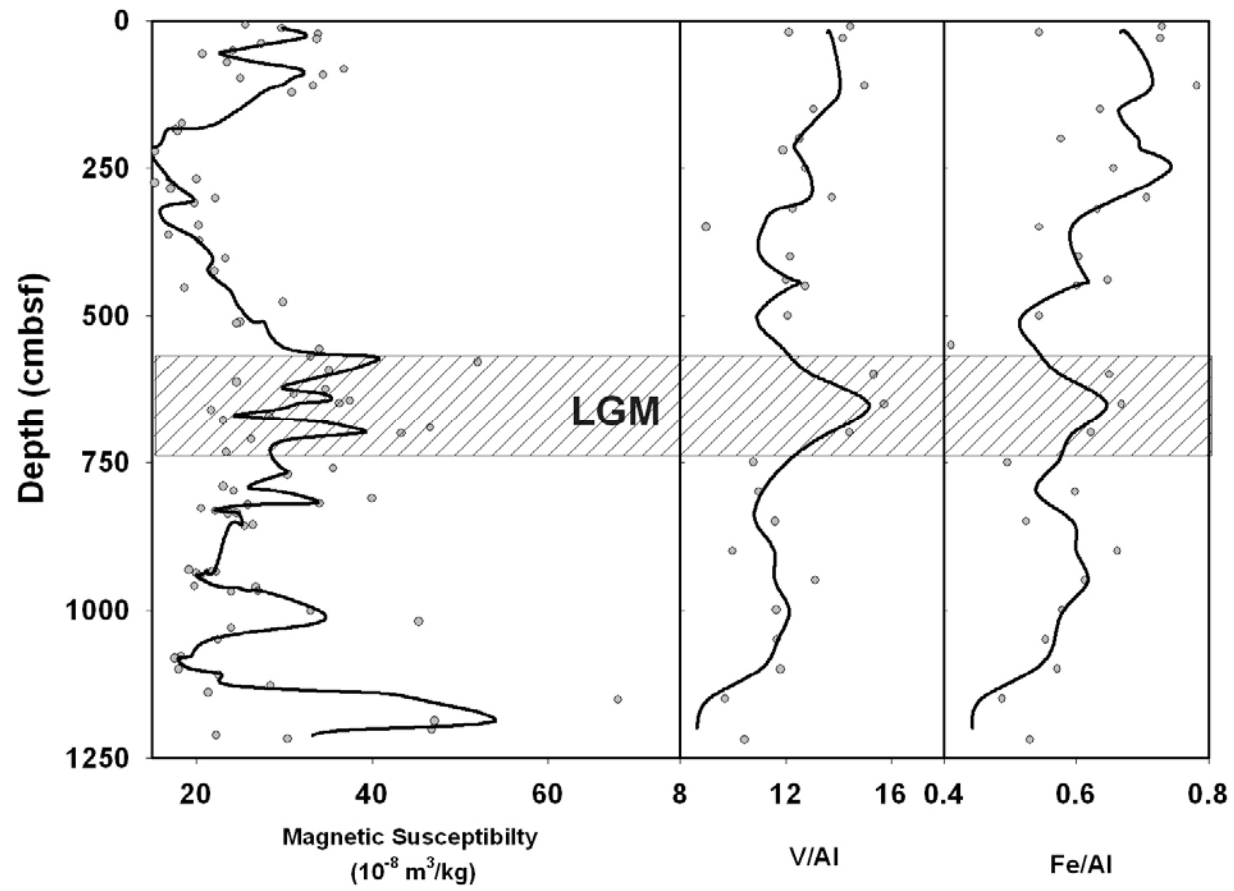


Fig. 4



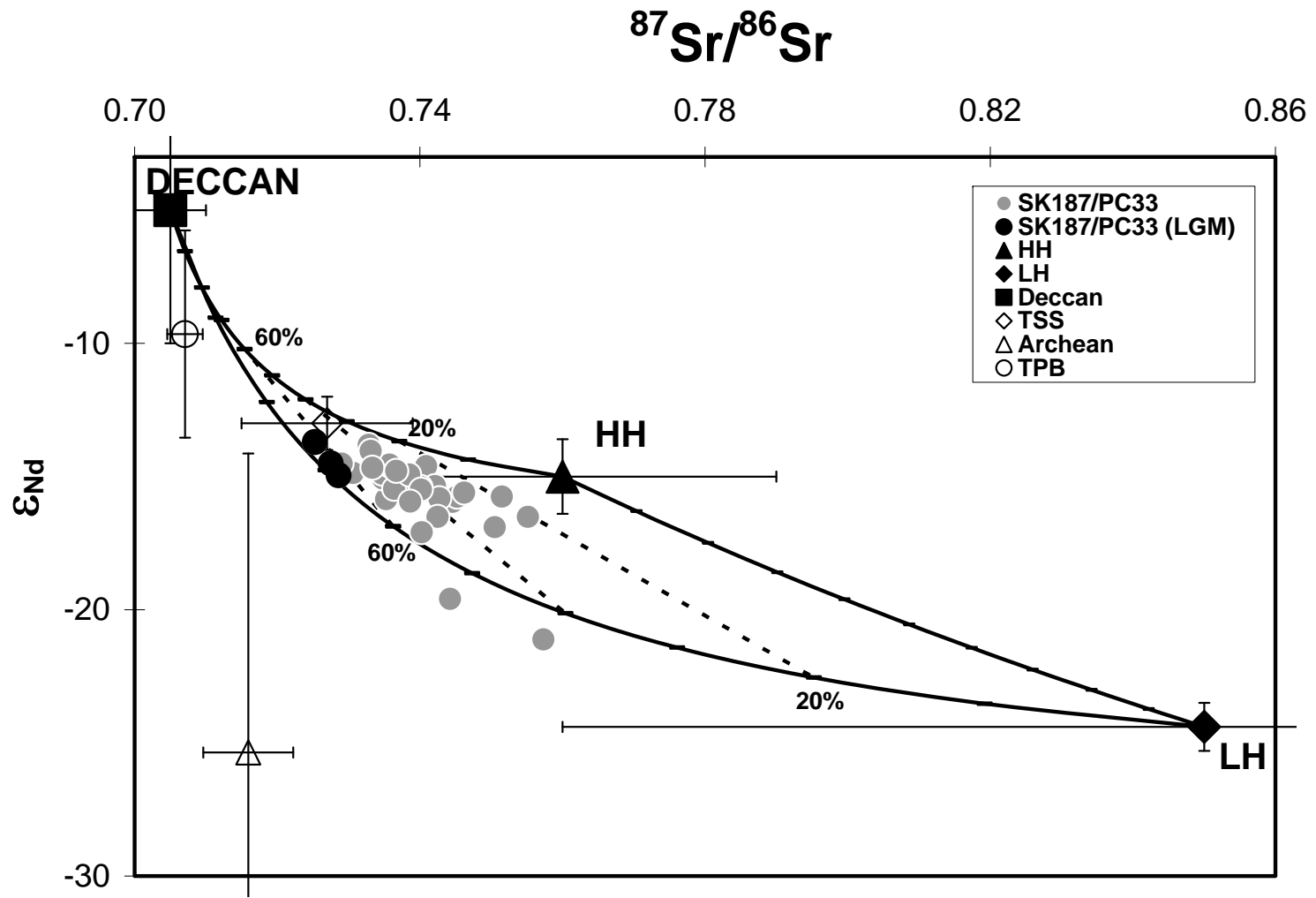


Fig. 5